ORIGINAL PAPERS

Synergistic effects of salt and ultraviolet radiation on the rice-field cyanobacterium *Nostochopsis lobatus* HKAR-21

Ashish P. Singh[1] · Amit Gupta[1] · Prashant R. Singh[1] · Jyoti Jaiswal[1] · Rajeshwar P. Sinha[1,2]

Abstract

Environmental variation has a significant impact on how organisms, including cyanobacteria, respond physiologically and biochemically. Salinity and ultraviolet radiation (UVR)-induced variations in the photopigments of the rice-field cyanobacterium *Nostochopsis lobatus* HKAR-21 and its photosynthetic performance was studied. We observed that excessive energy dissipation after UVR is mostly caused by Non-Photochemical Quenching (NPQ), whereas photochemical quenching is important for preventing photoinhibition. These findings suggest that ROS production may play an important role in the UVR-induced injury. To reduce ROS-induced oxidative stress, *Nostochopsis lobatus* HKAR-21 induces the effective antioxidant systems, which includes different antioxidant compounds like carotenoids and enzymes such as superoxide dismutase (SOD), peroxidase (POD), catalase (CAT), and ascorbate peroxidase (APX). The study indicates that *Nostochopsis lobatus* HKAR-21 exposed to photosynthetically active radiation + UV-A + UV-B (PAB) and PAB + NaCl (PABN) had significantly reduced photosynthetic efficiency. Furthermore, maximum ROS was detected in PAB exposed cyanobacterial cells. The induction of lipid peroxidation (LPO) has been investigated to evaluate the impact of UVR on the cyanobacterial membrane in addition to enzymatic defensive systems. The maximal LPO level was found in PABN treated cells. Based on the findings of this research, it was concluded that salinity and UVR had collegial effects on the major macromolecular components of the rice-field cyanobacterium *Nostochopsis lobatus* HKAR-21.

✉ Rajeshwar P. Sinha
  rpsinhabhu@gmail.com

1   Laboratory of Photobiology and Molecular Microbiology,
    Centre of Advanced Study in Botany, Institute of Science,
    Banaras Hindu University, Varanasi 221005, India

2   University Center for Research & Development (UCRD),
    Chandigarh University, Chandigarh, India

Graphical abstract
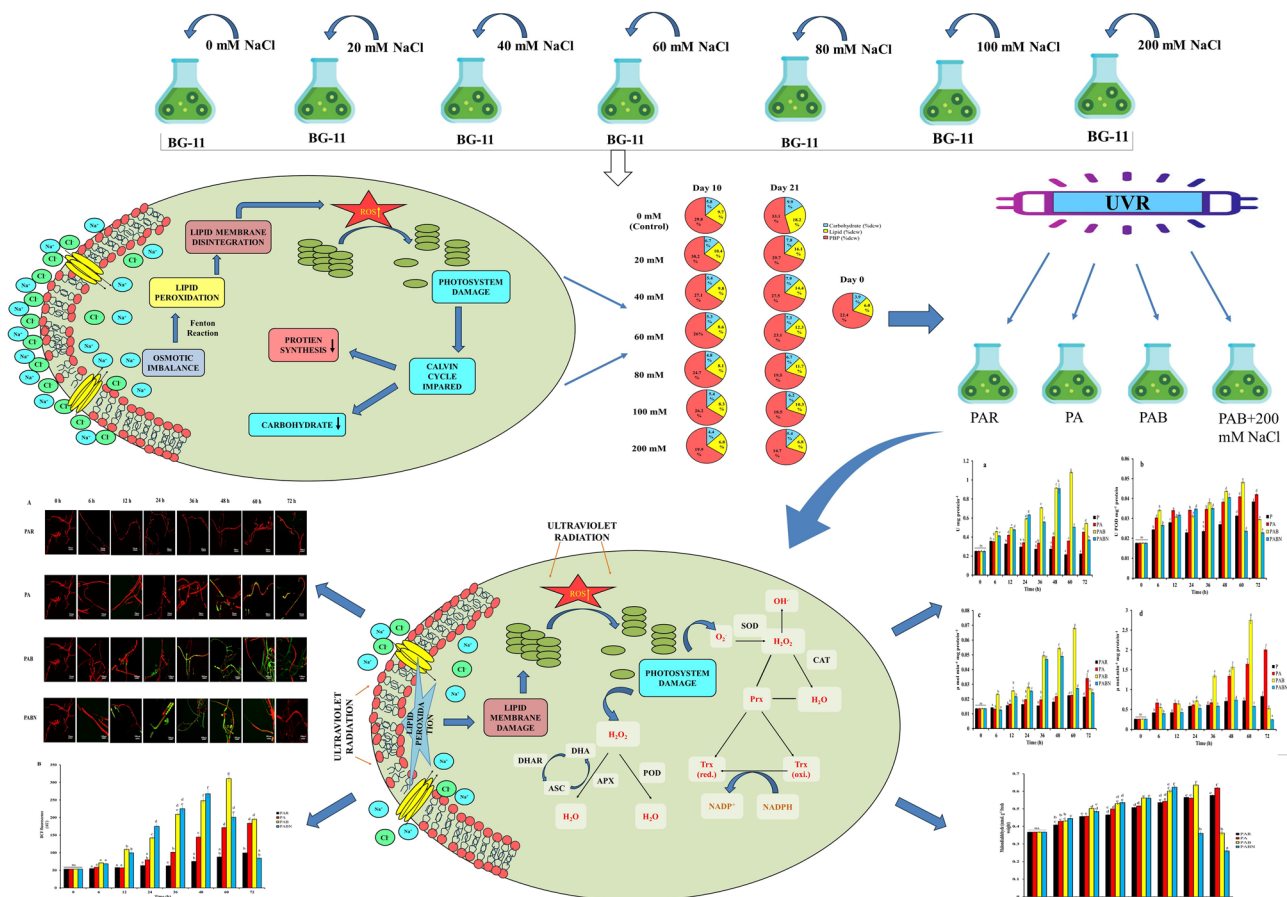
1 Introduction

Cyanobacteria are a unique group of prokaryotes that stand out for their contribution to the worldwide fixation of nitrogen and carbon dioxide [1, 2]. Regarding overall biomass and production in both aquatic and terrestrial environments, cyanobacteria are an essential component of microflora [3]. As food, fuel, and biofertilizers in paddy fields, they offer enormous potential for biotechnological uses [4]. In tropical paddy fields, the paramount importance of cyanobacteria in sustaining rice production has been recognized for a long time [5]. The adaptability of cyanobacteria to the physical, chemical and biological changes occurring in the rice ecosystem and their ability to fix nitrogen justifies the importance of the cyanobacteria. A special feature of cyanobacteria resides in the fact that they constitute a self-supporting system where the energy required for N_2 fixation is directly obtained through photosynthesis [6]. The independence of

cyanobacteria in relation to carbon and nitrogen, coupled with their great potential to withstand climatic variations, permits them to be ubiquitous and to make considerable contributions to the productivity of agricultural and other ecological habitats [7].

In the current world, climate changes and agricultural land degradation pose major challenges to crop productivity. Ultraviolet radiation (UVR) and rising salt stress are two of the main abiotic factors that significantly impact plant survival and growth. Currently, salt affects more than 1.2 billion hectares of land or around 6% of the world's total land surface [8]. Salt stress can cause more than $12 billion in annual economic losses worldwide [9]. Similar to how ozone depletion in the stratosphere is strongly influenced by climate change, rising greenhouse gas concentrations are also one of the major reasons behind increased influx of ultraviolet radiation (UVR), which harms photosynthetic ecosystems. Chlorofluorocarbons (CFCs) have dropped as a

result of the Montreal Protocol, but the ozone layer will not fully recover within this century [10, 11]. In recent times, salinization and climate change have affected almost all biological processes, including plant growth, photosynthesis, protein synthesis, and the metabolism of protein and phospholipids [12]. Similarly, the photosynthetic apparatus of cyanobacteria is comparable to that of higher plants, as the lipid content and overall membrane assembly of their thylakoid membranes and light-harvesting apparatus [13, 14]. Therefore, in order to research the processes of photosynthesis, membrane lipids, and signal transduction under abiotic stress, cyanobacteria might well be utilized as a model organism, which may also provide a useful model for higher plants [15].

Photosynthesis and nitrogen fixation are energy-intensive, ecologically significant processes that depend on capturing solar light [16]. In order to power both the photosystem (PS) PSI and PSII in cyanobacteria, the phycobilisome (PBS) (light-harvesting complex) of cyanobacteria gathers photosynthetically active radiation (PAR; 400–700 nm) of the solar spectrum [17]. Cyanobacteria are frequently exposed to deadly amounts of UV radiation (280–400 nm), which harms their photosynthetic apparatus because solar energy is a necessity for maintaining normal biochemistry and physiology of the cell [18]. To reduce the exposure of photopigments with UVR, cyanobacteria have a complementary chromatic adaptation, an ecologically significant phenomenon in which cyanobacteria may modify their pigment content in the PBS in response to ambient light quality [17, 19]. Cyanobacteria are damaged by UVR, particularly UV–B (280–315 nm), in a number of ways [20]. Direct consequences include DNA strand breakage, lipid peroxidation, thymine dimer formation-induced DNA damage, and impairment of orientation and motility [21–23]. Free radicals or reactive oxygen species (ROS) like hydroxyl radicals (HO$^•$), hydroperoxyl radicals (HO$_2^•$), hydrogen peroxide (H$_2$O$_2$), and superoxide anion radicals (O$_2^-$) are responsible for these changes [24, 25]. There are few publications on the impact of UVR on cyanobacteria's photosynthetic ability, despite the fact that several researches have demonstrated that UVR destroys photosynthetic components [26]. By causing photo-sensitizing reactions in the presence of Chl a and phycobilins, UV-A radiation indirectly impacts cells [27, 28]. UVR often targets PSII in photosynthetic species [29]. By photo-inactivating the oxygen-evolving complex or the D1 protein, UVR can directly harm PSII [30, 31].

Numerous studies have shown that the effects of UV-B radiation on photosynthetic species are detrimental and exceedingly diverse, affecting processes at all stages, from the molecular to the ecophysiological level [32]. According to certain studies, while largely harmful, UV-A and UV-B radiations appeared to have some beneficial effects in reducing photoinhibition or aiding the recovery of hindered

photosynthesis. In vivo Chl a fluorescence is a useful bioindicator for assessing the physiological condition of cyanobacteria during UVR. Also, maximum quantum yield and electron transport rate can be used as physiological stress markers in cyanobacteria [33, 34]. In the present study, we have assessed the variation in photopigments, their photosynthetic performance under UVR, and the effect of increasing salt concentration on total proteins, lipids, carbohydrate composition and phycobiliproteins (PBPs). The maximum quantum yield of dark-acclimated samples (optimum quantum yield: F_V/F_M), Non-Photochemical Quenching (NPQ), relative electron transport rate (rETR), the quantum yield of regulated energy dissipation in PSII (Y(NPQ)), and the quantum yield of non-regulated energy dissipation in PSII (Y(NO)), as determined by pulse amplitude modulated fluorescence (PAM) measurements, were monitored in order to study the photosynthetic performance of the cyanobacterium under different UV stress conditions. Thereafter, in UV treated cells, in vivo ROS was detected with the help of 2′,7′-dichlorodihydrofluorescein diacetate (DCFH-DA). During the organisms' exposure to UVR, the antioxidative enzymes such as superoxide dismutase (SOD), peroxidase (POD), catalase (CAT), and ascorbate peroxidase (APX) were examined. In addition to enzymatic defense systems, lipid peroxidation induction has been analyzed to see how UV radiation affects the cyanobacterial membrane.

2 Materials and methods

2.1 Experimental organism and growth conditions

The cyanobacterium *Nostochopsis lobatus* strain HKAR-21 (Accession no. OP656310) was isolated from rice-fields of Mau, Uttar Pradesh, India. Using a light microscope (Olympus CX21i, USA), the cyanobacterium's morphology was investigated. Cultures of *Nostochopsis lobatus* strain HKAR-21 were routinely cultivated photo autotrophically and axenically at 25 ± 2 °C in an autoclaved BG-110 medium [35]. Fluorescent tubes were used to illuminate cultures at a photon flux density of 55.08 ± 9.18 µmol m^{-2} s^{-1} for 14 h, followed by 10 h of darkness. To prevent contamination, the cultures have been subcultured at regular intervals. Every experiment was carried out in cultures that grew exponentially or logarithmically over a period of 17 days.

2.2 Sequencing and phylogenetic analyses

The *16S rDNA* gene was amplified for molecular characterization, and the maximum likelihood approach was applied to evaluate phylogenetic tree mapping. The alignment of *16S rDNA* gene fragment sequences with known sequences obtained in the GenBank database was done using

the BLAST software of the NCBI search [36]. ClustalW software was used to accomplish multiple alignments. The *16S rDNA* gene sequence of the cyanobacterium was then classified into a phylogenetic group in accordance with Desikachary's [37] taxonomy in order to examine the genetic diversity both within and between the groupings. After that, a phylogenetic tree was created using MEGA-11's neighbour-joining technique [38, 39].

2.3 Experimental setup

Initially, several exogenous NaCl concentrations (0 (control), 20, 40, 60, 80, 100, and 200 mM) were applied in the BG-110 medium for screening purposes. For LD_{50} determination, the experiment was conducted under a light intensity of 55.08 ± 9.18 μmol photons $m^{-2} s^{-1}$ at 25 ± 2 °C with 14:10 light/dark cycles for 21 days. NaCl (200 mM concentration) was found to be lethal for the development of the rice-field cyanobacterium *Nostochopsis lobatus* strain HKAR-21. Therefore, it was used together with UVR for the further experiments. Afterwards, in sterile glass Petri dishes (120 mm in diameter), the uniform cultures of the exponentially growing *Nostochopsis lobatus* strain HKAR-21 (150 mL of culture with OD 750 nm $= 0.72 \pm 0.02$; Path length 1 cm) were taken and subjected to artificial photochemical active radiation (PAR), PAR + UV-A (PA), and PAR + UV-A + UV-B (PAB) radiation in a UV chamber with and without exogenous addition of 200 mM NaCl (PABN) (Merck, S9888). The cells were transferred and then exposed to a consistent amount of PAR (55.08 ± 9.18 μmol photon $m^{-2} s^{-1}$) (OSRAM L 36 W: 32 Lumilux de luxe warm white and Radium NL 36 W: 26 Universal white, Germany), UV-A (15 μmol photon $m^{-2} s^{-1}$) (Philips Ultraviolet-A TL 15 W:12, Holland), and UV-B (6.5 μmol photon $m^{-2} s^{-1}$) (Philips Ultraviolet-B TL 15 W:12, Holland) lights for 72 h at a temperature of about 25 ± 2 °C to avoid excessive heating of cells. Different cut-off filter foils, such as 320 nm (Folex, Dreieich, Munich, Germany), 395 nm, and 295 nm (Ultraphan, Digefra, Munich, Germany), were placed on the Petri dishes in order to obtain transmittance of the appropriate wavebands of PAR (400–700 nm), UV-A (315–400 nm), and UV-B (280–315 nm), respectively. For the analysis, equal triplicate samples were taken from each filter treatment at predetermined intervals of 0 (control), 6, 12, 24, 36, 48, 60, and 72 h.

2.4 Determination of total protein and pigment contents

The colorimetric approach given by Lowry et al. (1951) was used to assess the total protein concentration [40]. Samples (2 mL) were taken and centrifuged for 10 min at 10,000 rpm at 4 °C. After being washed twice with sterile, double-distilled water, the pellets underwent additional processing to extract and measure the total proteins. Pellets were treated with 1.8 mL of alkaline reagent C, which was prepared by combining reagents A and B in a 50:1 ratio (Reagent A: 0.1 N NaOH + 2% Na_2CO_3; Reagent B: 0.5% $CuSO_4.5H_2O$ in 1% sodium potassium tartrate) and 200 μL of 50% Folin–Ciocalteau reagent in water (Merck, 109,001). Then, solutions were mixed properly with the help of a vortex. After that, the samples were left at room temperature in the dark for 30 min. The color intensity was quantified at 660 nm, and the concentration of the protein content was estimated by using 1 mg mL^{-1} standard of bovine serum albumin (BSA) (Himedia, India).

To determine the pigment concentration, samples were homogenized in 100% methanol (Merck, 106,009). The samples were kept at 4 °C overnight and then centrifuged at 10,000 rpm for 10 min. Using quartz cuvettes and a double-beam spectrophotometer (UV-2900, Schimadzu, Tokyo, Japan), the absorption spectra of the supernatants were detected over the wavelength range of 200–700 nm. Maximum absorbance was seen for both Chl *a* and total carotenes at 666 nm and 470 nm, respectively. The procedures outlined by Şükran et al. [41] were used to determine Chl *a* and total carotene levels.

By using the following equation,

$$Chl\ a = 15.65\ A_{666} - 7.340\ A_{653}$$
$$C_{x+c} = 1000\ A_{470} - 2.860\ Ca - 129.2\ Cb/245$$

where Ca = Chl *a*, Cb = Chl *b*, C_{x+c} = Total carotene and Chl *b* = 0 (In cyanobacteria Chl *b* is absent).

2.5 Isolation and quantification of PBPs

Cell samples were centrifuged at 10,000 rpm for 10 min at 4 °C. The pellets were then re-suspended in the same buffer with a reaction mixture consisting of 1 mM EDTA, 1 mM phenylmethanesulfonylfluoride fluoride (PMSF), and 5% (w/v) sucrose after being rinsed twice with phosphate buffer (PB, 50 mM). Thereafter, cells were periodically sonicated for three cycles of 2 min at the brake of 1 min (130W, 20 kHz, 50% amplitude) respectively. Suspended aliquots were repeatedly frozen and thawed at -20 °C and 4 °C, respectively, for successful PBPs extraction [42]. The amount of PBP was estimated by UV–Vis spectrophotometer (UV-2900, Schimadzu, Tokyo, Japan) by using an equation described by Bennett and Bogorad, 1973 [43].

$$PC\ (mg\ mL^{-1}) = (A_{615} - 0.474 * A_{652})/5.34$$
$$APC\ (mg\ mL^{-1}) = (A_{652} - 0.208 * A_{615})/5.09$$
$$PE\ (mg\ mL^{-1}) = [(A_{562} - (2.41(PC) - (0.849 * APC)]/9.62$$
$$Total\ PBP = PC + APC + PE$$

2.6 Lipids and carbohydrate estimation

Total lipid from the samples was extracted by using a modified Bligh and Dyer extraction method [44]. The salt-treated cyanobacterial culture (50 mL) was centrifuged for 10 min at 6500 rpm. After removing the supernatant, the cyanobacterial biomass was separated, rinsed with double distilled water, and centrifuged once more. Then pellet was oven-dried overnight at 70ºC, and the weight of the biomass was measured. After that, cyanobacterial biomass (g), methanol (mL) and chloroform (mL) were mixed in a ratio of 1:2:1 and incubated for 18 h at 25 ± 1ºC. The mixture was then vortexed for 2 min and again for 1 min after adding 1 mL of chloroform. After that, 1 mL of double distilled water was added to the mixture and quickly vortexed again for 2 min. Different layers were separated by centrifugation at 3000 rpm for 10 min, and the lowest lipid layer that contained the chloroform was gently removed and transferred to a sterile, preweighed centrifuge tube (W1). Then the chloroform phase was evaporated in a water bath at 70ºC for 20 min. Once more, the centrifuge tube's weight was taken (W2), W1 and W2 were subtracted and divided by dried cyanobacterial biomass to calculate the lipid content. Finally, the result was multiplied by 100 before being represented as % dry cell weight (dcw). The amount of total carbohydrates was analyzed by using the Dubois phenol–sulfuric acid method [45]. For that, 5 mL salt-treated cultures were taken and centrifuged for 10 min at 10,000 rpm at room temperature, followed by washing with double distilled water. Then after, 50 µL of phenol (80%) (Merck, India) and 5.0 mL of concentrated sulfuric acid were added to the samples and mixed vigorously before incubation in a water bath at 25–30 °C. The color intensity was measured at 490 nm using a UV–Visible spectrophotometer, and quantification of the carbohydrate was done by using 1 mg mL^{-1} glucose as a standard (Millipore, 108,337).

2.7 Photosynthetic performance measurements

Using a pulse-amplitude-modulation (PAM) fluorometer (PAM-2500, Walz, Effeltrich, Germany), the photosynthetic efficiency of *Nostochopsis lobatus* HKAR-21 under PAR, PA, PAB, and PABN-treated samples was assessed after 0, 6, 12, 24, 36, 48, 60, and 72 h of exposure. Firstly, 2 mL samples were subjected to modulated light (0.1 µmol m^{-2} s^{-1}) after being dark-adapted for 15 min at room temperature. Then, a light-emitting diode was used to measure the minimal fluorescence yield (F_O). By delivering a saturating pulse of 3000 µmol photons m^{-2} s^{-1} for 0.3 s, the maximum fluorescence yield (F_M) was determined. After that, photochemistry was induced, and the steady-state condition (F_S) was obtained using red actinic light of 101 µmol photons m^{-2} s^{-1}. To assess the light-adapted maximum fluorescence yield (F_M'), a second saturating pulse at 3000 µmol photons m^{-2} s^{-1} was administered during the induction phase. Furthermore, the minimum fluorescence generation in the light-adapted state (F_O') was quantified under 5 µmol photons m^{-2} s^{-1} of far-red irradiation at the conclusion of the induction phase, immediately following the switching off of the actinic light. Based on the measured values of F_O, F_M, F_O', F_M' and F_S, the PamWin 3.20 program automatically calculated the effective quantum yield of photochemical energy conversion in PSII (Y(II)), relative electron transport rate (rETR), the quantum yield of regulated energy dissipation in PSII (Y(NPQ)), and the quantum yield of nonregulated energy dissipation in PSII (Y(NO)). In order to calculate these parameters, PamWin software uses the following equations- [46–50].

$$Y(II) \text{ or } F_V/F_M = F_M - F_O / F_M$$

where F_V/F_M represents the effective quantum yield of photochemical energy conversion in PSII.

$$rETR = \phi PSII \times irradiance \times 0.5,$$

Relative electron transport rate (rETR) was measured according to Rascher et al. [51] and Klughammer and Schreiber [52].

$$Y(NPQ) = (F_S/F_M') - F_S/F_M,$$

$$Y(NO) = F_S/F_M$$

2.8 Estimation of antioxidant enzymes activity

After the desired intervals of UV exposure, cyanobacterial cell suspensions were collected and centrifuged at 12,000 rpm for 20 min at 4 °C and with the aid of sonication (Sonic and Materials, USA) pellet was homogenized in extraction buffer (consisting of 50 mM PB (pH 7.5), 2.5 mM phenylmethyl sulfonyl fluoride (PMSF), 1 mM ethylenediaminetetraacetic acid (EDTA), 1% (w/v) polyvinyl polypyrollidone (PVP). After that, the homogenate was centrifuged again for 10 min at 10,000 rpm at 4 °C and the supernatant was used as the reaction mixture for the enzyme test [53]. Initially, after incubation in darkness for 1 min, the O_2 released and H_2O_2 absorbance at 240 nm ($\varepsilon = 39.4$ mM^{-1} cm^{-1}) were measured to assess the catalase (CAT, EC 1.11.1.6) activity [54, 55]. The activity of superoxide dismutase (SOD, EC 1.15.1.1) was assessed by measuring the inhibition of nitro blue tetrazolium (NBT) at 560 nm [56]. Peroxidase activity (POD, EC 1.11.1.7) was measured by assessing the production of purpurogallin from pyrogallol by taking absorbance at 420 nm at 20 °C [57]. The conversion of ascorbate into monodehydroascorbate at 290 nm ($\varepsilon = 2.8$ mM^{-1} cm^{-1}) was analyzed to determine the ascorbate peroxidase's (APX, EC 1.11.1.11) activity [58]. Then, a spectrophotometric

technique described by Kampfenkel in 1995 was used to determine the ascorbate content [59].

2.9 Estimation of lipid peroxidation

Cyanobacterial samples were homogenized in 100 mM phosphate buffer (pH = 7.0) and centrifuged at 15,000 rpm for 10 min. Lipid peroxidation level was estimated in terms of malondialdehyde (MDA) content as given by Heath and Packer (1968) [60]. Four mL of 0.5% Thiobarbituric acid (TBA) in 20% Trichloroacetic acid (TCA) and 2.0 mL of the supernatant were mixed. Then the mixture was heated at 95 °C for 30 min and immediately cooled in an ice bath. After that, the mixture was centrifuged for 10 min at 10,000 rpm to measure the absorbance of the supernatant at 532 nm. The value of non-specific absorbance at 600 nm was subtracted. Finally, using its $155\ nmol^{-1}\ cm^{-1}$ absorption coefficients, the MDA concentration was determined and represented as nmol (MDA) g^{-1} fresh weight.

2.10 Reactive oxygen species (ROS) measurement

ROS measurement was done using a fluorescence microscope and a DCFH-DA dye (Sigma-Aldrich, India). Initially, a 2 mM stock solution of DCFH-DA in ethanol was prepared, which was stored at -20 °C in the dark. Then, samples were treated with a 15 μM final concentration of dye; after that, all samples were incubated for 1 h in the dark at room temperature with continuous shaking. The fluorescence of the samples was measured using a fluorescence spectrophotometer (Cary eclipse, Agilent Technologies) with an excitation wavelength of 485 nm and an emission band of 525 nm at room temperature. Fluorescence was assessed in terms of emitted fluorescence intensity following various periods of stress exposure [25]. Thereafter, imaging was done using the Nikon 90i Eclipse microscope. The image was acquired in epifluorescence mode using a 20 × and 100 × objectives in a dark room equipped with blue (FITC) and green (TRITC) filters. Then, NIS elements AR software 4.0 was used for image analysis. To avoid photooxidation of the dye, the whole ROS estimate process, from sample collection to imaging, was carefully carried out in low light. The red autofluorescence of photosynthetic pigments (Chl *a* and PC) and the green fluorescence of dichlorofluorescein (DCF) were measured using TRITC and FITC, respectively. Finally, green and red fluorescence originating from cells (3 replicates for each treatment) were used to measure ROS levels. Green/red (G/R) ratios were used to depict ROS levels, with a larger G/R ratio signifying increased ROS production [61, 62].

2.11 Statistical analysis

The sum of the mean values ± standard deviation (SD) of three biological replicates ($n = 3$) is used to represent all data. Each replicate microscope picture of a total cells was evaluated for ROS estimate. The data are displayed as means of total cells' measurement ± SD. When a significant difference was found, all data were subjected to a two-way Analysis of variance (ANOVA) analysis, and a *post-hoc* multiple comparisons analysis using the Tukey test was carried out (IBM SPSS statistics version 16.3, Chicago, IL, USA). The degree of significance (α) for each test was set at 0.05.

3 Results

Based on microscopic examination, morphological identification, molecular characterization and phylogenetic tree mapping, the cyanobacterium was identified as *Nostochopsis lobatus* HKAR-21. The cyanobacterium's *16S rDNA* gene sequence was submitted to the NCBI database under accession number OP656310. The phylogenetic tree showed that *Westiellopsis prolifica* GBBB09 (accession number MT792729) is the closest homologue of *Nostochopsis lobatus* HKAR-21 (Fig. 1). It is found to be a filamentous and heterocystous cyanobacterium, a member of the order Nostocales and family Hepalosiphonaceae.

3.1 Total protein and pigment

The salt stress negatively influences the photopigments and productivity of rice-field cyanobacterium *Nostochopsis lobatus* HKAR-21. The effects of different salt concentrations on pigments and total proteins are shown in the Supplementary Table S1. As compared to the control, Chl *a*, carotenoids, and total protein content of *Nostochopsis lobatus* HKAR-21 showed 66%, 64.3% and 56.4% depletion ($p < 0.05$) after 21 days of 200 mM NaCl treatment, respectively (Supplementary Table S1).

Thereafter, the effect of different radiation conditions (i.e., PAR, PA, PAB and PAB + NaCl (200 mM) (PABN)) on the photopigments and protein content of *Nostochopsis lobatus* HKAR-21 was measured, which has been summarized in Table 1. PAR and PA irradiated cells showed the optimum increment in Chl *a*, carotene and total protein concentration; however, in PAB and PABN irradiated cells, a significant decrease was observed with the highest inhibition in PABN. The Chl *a* and total protein content of *Nostochopsis lobatus* HKAR-21 showed 72% and 58% depletion after 72 h of PAB and PABN treatment, respectively, compared to the controls. A two-fold increase in Chl *a* was observed after 72 h of PAR treatment, as well as 33.5% increase in protein content, was also determined. Subsequently, in PA-treated cells, 66% and

Fig. 1 Phylogenetic relationship of the rice-field cyanobacterium *Nostochopsis lobatus* HKAR-21. The maximum composite likelihood approach was used to calculate the evolutionary distances of isolated cyano-bacterium. The cyanobacterial species shown in green belongs to Stigonematales order and all the other species shown in black were member of Nostocales order. The isolated rice-field cyanobacterium is shown in red color
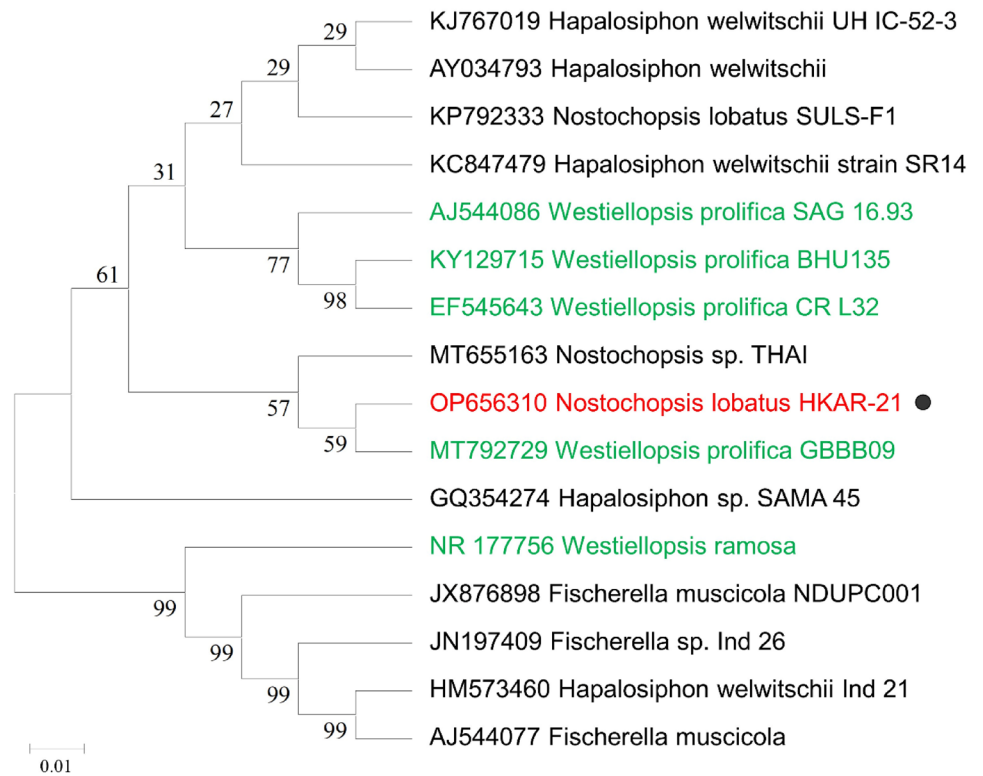

Table 1 Chl *a*, total carotene and total protein contents of rice field cyanobacterium *Nostochopsis lobatus* HKAR-21 exposed to PAR, PAR + UV-A (PA), PAR + UV-A + UV-B (PAB) and PAR + UV-A + UV-B + NaCl (200 mM) (PABN)

Time (h)	Chl *a* ($\mu g\ mL^{-1}$) (mean ± SD)				Total Carotene ($\mu g\ mL^{-1}$) (mean ± SD)			
	PAR	PA	PAB	PABN	PAR	PA	PAB	PABN
0	9.19 ± 0.053	9.19 ± 0.053	9.19 ± 0.053	9.19 ± 0.053	641.05 ± 3.64	641.05 ± 3.64	641.05 ± 3.64	641.05 ± 3.64
6	9.94 ± 0.037	9.60 ± 0.021	9.33 ± 0.0370	8.95 ± 0.0161	694.57 ± 3.05	641.54 ± 0.94	752.81 ± 33.14	739.84 ± 3.77
12	10.34 ± 0.029	10.22 ± 0.191	9.60 ± 0.0214	8.43 ± 0.0147	683.74 ± 2.44	683.44 ± 2.05	826.53 ± 13.83	805.71 ± 3.45
24	10.67 ± 0.036	11.03 ± 0.024	8.77 ± 0.0265	8.48 ± 0.021	720.82 ± 1.07	589.45 ± 1.07	973.92 ± 15.54	877.28 ± 1.88
36	11.41 ± 0.029	11.79 ± 0.064	7.39 ± 0.0595	6.55 ± 0.053	874.71 ± 2.97	847.61 ± 1.52	1027.46 ± 11.46	957.09 ± 2.96
48	14.10 ± 0.030	12.49 ± 0.028	6.04 ± 0.0661	4.94 ± 0.1184	905.89 ± 2.56	802.94 ± 1.51	1099.15 ± 9.75	1011.43 ± 8.26
60	16.67 ± 0.034	14.13 ± 0.013	4.16 ± 0.0096	3.32 ± 0.1502	932.35 ± 2.97	1095.92 ± 1.50	1055.92 ± 6.71	1026.73 ± 5.17
72	18.67 ± 0.074	15.24 ± 0.302	2.60 ± 0.0096	1.27 ± 0.0244	1080.07 ± 6.0	1199.98 ± 3.42	1074.43 ± 1.48	908.16 ± 4.62

Time (h)	Total Protein ($\mu g\ mL^{-1}$) (mean ± SD)			
	PAR	PA	PAB	PABN
0	203.87 ± 3.05	203.87 ± 3.05	203.87 ± 3.05	203.87 ± 3.05
6	212.6 ± 1.25	208.6 ± 5.30	201.73 ± 1.15	184.07 ± 1.15
12	217.47 ± 9.02	213.2 ± 3.46	189.13 ± 2.31	179.6 ± 2.0
24	223.67 ± 4.62	217.87 ± 1.10	172.73 ± 8.33	175.2 ± 4.0
36	241.47 ± 5.03	221.73 ± 1.15	158 ± 3.46	165.73 ± 4.16
48	258.33 ± 4.62	224.67 ± 5.03	142.93 ± 3.05	147.07 ± 2.31
60	261.87 ± 3.05	241.2 ± 3.46	110.2 ± 3.46	104.4 ± 5.30
72	271.8 ± 3.46	246.53 ± 8.08	85 ± 2.02	61.13 ± 3.05

21% increment was found in Chl *a* and total protein after 72 h of treatment, respectively. However, the total carotene content was found to be increased by 68% and 87% after 72 h of PAR and PA treatment, respectively. Nevertheless, in PAB-irradiated cells, carotene level was increased by 68% after 72 h of irradiation. Similarly, in PABN irradiated cells, the carotene level was increased up to 60% after 60 h of irradiation; after that, it depleted slightly, as shown in Table 1.

3.2 Total carbohydrate, lipid and PBP content

All three macromolecular components of the cells were found to have increased significantly after 21 days of growth under control conditions. However, a small difference was observed in 20 and 40 mM NaCl-treated cells, but all three components were reduced significantly in the 200 mM NaCl-treated samples (Fig. 2). Notably, as shown in Supplementary Table S2, after 21 days of treatment, a decrease of 48.5% was found in the carbohydrate content of 200 mM NaCl treated sample, as well as total lipid was also deprived by 63%, as compared to the control. Similarly, about a 50% decrease in phycobiliproteins (PBPs) content was observed after 21 days of treatment (Fig. 2).

Fig. 2 Percentage composition of phycobiliproteins (PBPs), carbohydrate and lipid in the biomass of *Nostochopsis lobatus* HKR-21 under different salt (NaCl) concentrations. The percentage composition of PBPs, carbohydrate and lipid in the biomass was calculated at 0 days and after 10 and 21 days of growth under different salt (NaCl) concentrations
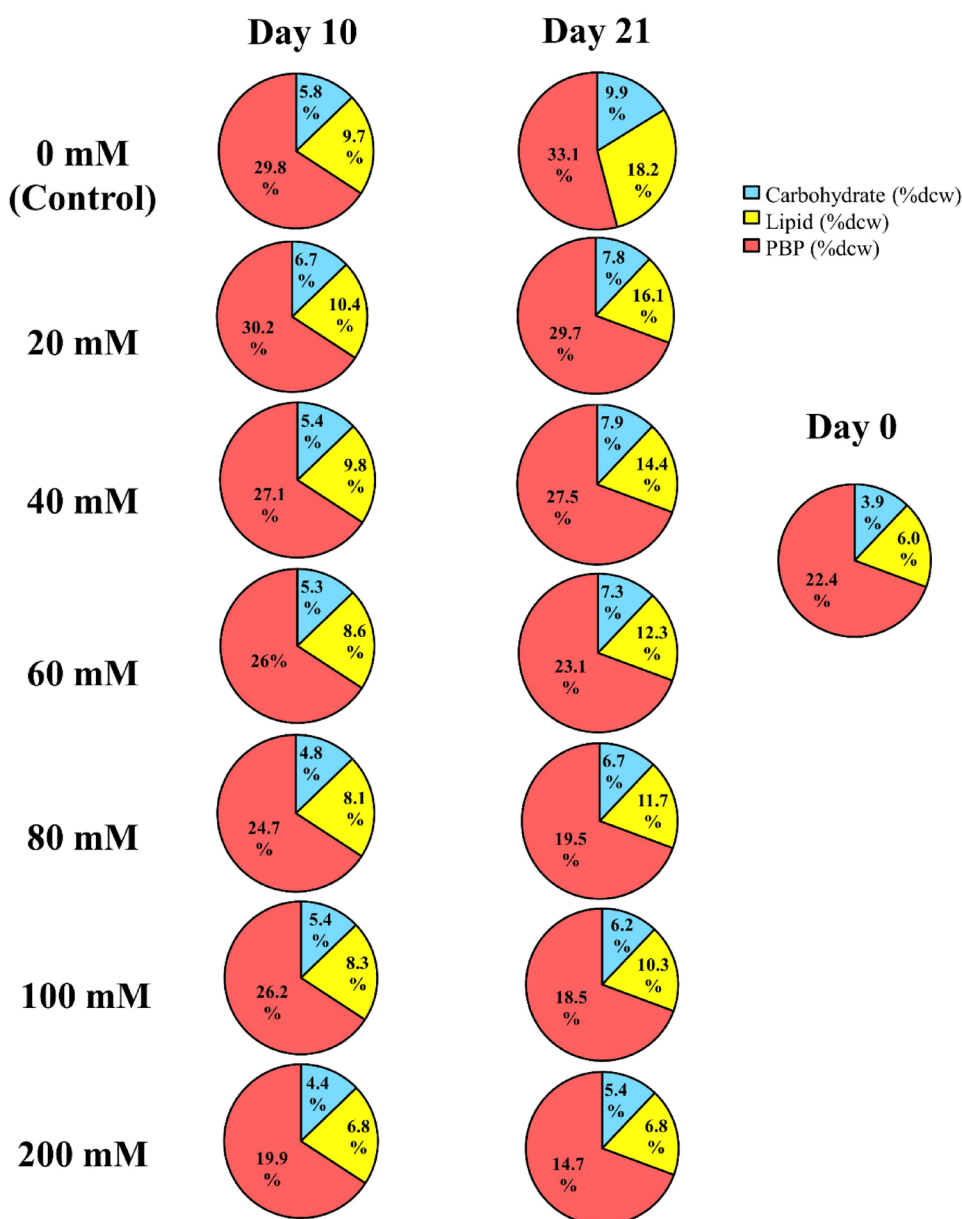
Table 2 F_V/F_M of rice field cyanobacterium *Nostochopsis lobatus* HKAR-21 exposed to PAR, PA, PAB and PABN irradiation at different time intervals up to 72 h

Time (h)	PAR	F_V/F_M (mean ± SD)		
		PA	PAB	PABN
0	0.415 ± 0.0025	0.415 ± 0.0025	0.415 ± 0.0025	0.415 ± 0.0025
6	0.435 ± 0.0055	0.443 ± 0.0055	0.410 ± 0.0065	0.380 ± 0.0031
12	0.451 ± 0.0015	0.474 ± 0.0045	0.375 ± 0.006	0.343 ± 0.0012
24	0.462 ± 0.0045	0.490 ± 0.0015	0.294 ± 0.0031	0.296 ± 0.0044
36	0.511 ± 0.0021	0.495 ± 0.0038	0.238 ± 0.0025	0.188 ± 0.0058
48	0.530 ± 0.0070	0.525 ± 0.0057	0.181 ± 0.0075	0.093 ± 0.0025
60	0.554 ± 0.0036	0.543 ± 0.006	0.099 ± 0.0017	0.024 ± 0.0021
72	0.582 ± 0.0021	0.560 ± 0.0057	0.037 ± 0.0027	0.003 ± 0.0052

3.3 Photosynthetic performance and quenching coefficients

As indicated in Table 2, the variations in the maximum quantum yield of the photosynthetic apparatus (F_V/F_M) of the *Nostochopsis lobatus* HKAR-21 were measured under PAR, PA, PAB, and PABN stress conditions. A substantial reduction in F_V/F_M was found in both PAB and PABN irradiated samples, with exposure to PABN causing maximum inhibition. F_V/F_M decreased significantly ($p < 0.05$) by 91% and 99% under PAB and PABN irradiation, respectively, after 72 h. However, after 72 h of PAR and PA irradiation, respectively, it was discovered that the maximum quantum yield of the photosynthetic apparatus (F_V/F_M) had risen ($p < 0.05$) concurrently by 40% and 35% (Table 2).

In all samples, the rETR rose with rising light levels until it eventually reached a saturation threshold before decreasing at higher light levels. Under various lighting conditions, the rETR behaved in a manner resembling the maximum quantum yield of the photosynthetic apparatus (F_V/F_M). The relative electron transport rate (rETR) in cells exposed to PAR radiation peaked 72 h after exposure (Fig. 3a), and following exposure to PA radiation, a nearly identical pattern was seen (Fig. 3b). Although rETR was found to be the highest after 6 h of PAB induction, it decreased sharply with the time period (Fig. 3c). Similarly, the PABN treated cells showed the maximum value of rETR after 24 h of induction, but it dropped quickly to the lowest after 48 h of induction (Fig. 3d).

Curves of quenching coefficients, Y(NPQ) and Y(NO), showed variations with different irradiations (i.e., under PAR, PA, PAB and PABN) and with enhanced levels of actinic irradiance, the sample's Y(NPQ) values decreased linearly (Fig. 3e–h). Although, the maximum drop was observed in the PABN irradiated samples (Fig. 3h). Contrastingly, the Y(NO) was found to be increased with time as well as different irradiation conditions. In PAR and PA irradiated cells, Y(NO) was continuously increased from 0 to 72 h (Fig. 3i, j). However, in PAB and PABN irradiated cells, the value of Y(NO) increased very sharply (Fig. 3k, l). PAB radiation led to a significant increase in Y(NO) values which increased continuously up to 72 h. However, the maximum effect was observed in PABN irradiated cells after 72 h in comparison to the control.

3.4 In vivo detection of ROS

Fluorescence microscopy and spectrophotometry were used to detect in vivo free radical generation in the cells of the filamentous cyanobacterium *Nostochopsis lobatus* HKAR-21 after varying exposure times to PAR, PA, PAB, and PABN radiations. Figure 4a shows that, in comparison to the controls, there were substantial variations in the PA, PAB, and PABN radiations, which led to an increase in the production of free radicals as evidenced by green fluorescence. The emission spectra of samples incubated with DCFH-DA after varying exposure times to PAR, PA, PAB, and PABN are shown in Fig. 4b. The highest levels of ROS were observed in the samples that had been exposed to PAB. As compare to PAR, 6.5-fold ($p < 0.05$) increase was found in the DCF-fluorescence after 60 h of PAB-treatment (Fig. 4b). Although, there was a slight difference in DCF fluorescence observed between samples treated with PAR and PA (Fig. 4b). Similar to this, as shown in Fig. 4a, under the PABN stress condition, the production of free radicals increased along with the duration of the stress up to 48 h. Following that, a decrease in fluorescence was found as a result of the salt's effects on the cyanobacterium's photopigments activity (Fig. 4a).

Additionally, Supplementary Fig. S1 shows the DCF and chlorophyll auto-fluorescence, green and red ratio (G/R) of cyanobacterium treated with PAR and different radiations of UVR (i.e., PA, PAB, PABN). Furthermore, similar trend was observed in G/R ratio of the cyanobacterium. PAB treated cells showed significant increase of 23-fold ($p < 0.05$) in G/R ratio as compared to control. However, PABN treated cell showed significant upliftment of 21-fold ($p < 0.05$) up to
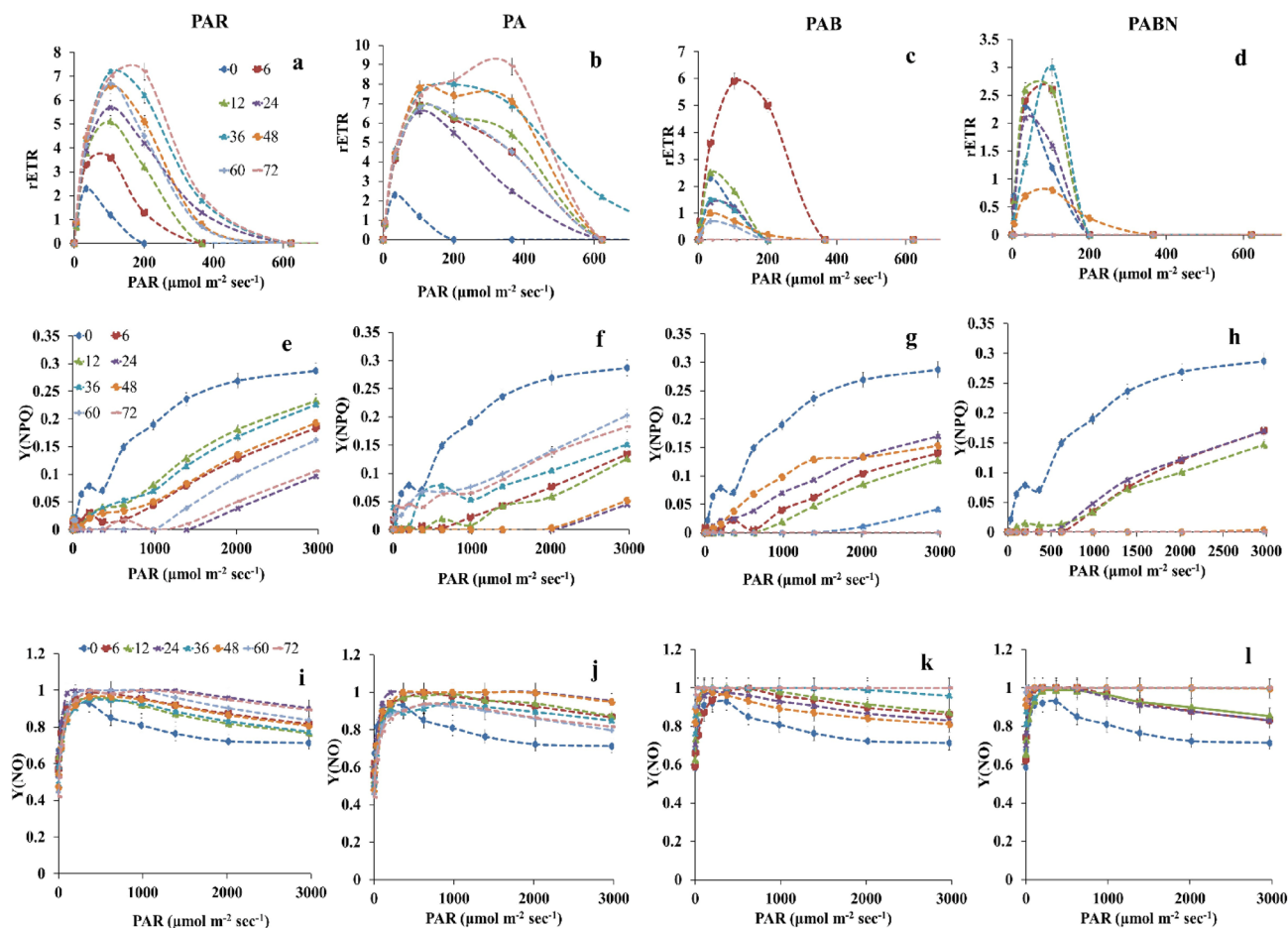
Fig. 3 Variability in relative electron transfer rate (rETR), the quantum yield of regulated energy dissipation in PSII (Y(NPQ)) and the quantum yield of nonregulated energy dissipation in PSII (Y(NO)) of *Nostochopsis lobatus* HKAR-21 cultures exposed to PAR, PA, PAB and PABN irradiation for varying time periods (in hours). The error bar indicates the standard deviation of mean (means ± SD, $n = 3$)

48 h of irradiation. Thereafter, G/R ratio was decreased due to impairment of the cells. Thus, it can be concluded from the fluorescence spectroscopy and microscopy results that PAB radiation had a far greater impact on ROS formation than PAR and PA radiations. ROS levels dramatically rose under PABN stress conditions, but were soon declined due to cell damage.

3.5 Antioxidant enzyme activity estimation

Cyanobacterium exposed to PAR, PA, PAB and PABN showed substantial changes in the activity of SOD, POD, CAT and APX (Fig. 5). In PAR irradiation, the SOD activity increased slightly at the beginning (6 h) and then went down continuously to 0.223 ± 0.006. Similarly, SOD activity increased 1.8-fold ($p < 0.05$) after 72 h of PA administration compared to the control. However, PAB significantly enhanced the SOD activity and was stimulated for up to 72 h. In PAB-treated samples compared

to controls, its activity increases by 4 times ($p < 0.05$). However, maximum SOD activity was found up to 60 h; after that, it decreased to at 72 h. Like PAB-treated cells, the SOD activity of the PABN-treated sample was found to be increased by 3.6 folds. Although the maximum SOD activity was observed after 60 h of treatment, after that it decreased sharply. As shown in Fig. 5a.

POD activity was 0.0176 ± 0.0004 U mg^{-1} of protein in control. It increased 2.17-folds after 72 h of PAR exposure (Fig. 5b). After 24 h of PAR exposure, there was a modest decline in POD activity. But following that, it keeps rising. In the case of PA exposure, POD activity steadily increased, and after 72 h of treatment, induction of up to 2.4-fold ($p < 0.05$) was seen. However, the significant rise in response to PAB exposure reached a maximum induction of 2.8 ($p < 0.05$) fold after 60 h of treatment. A decrease in POD activity resulted from more irradiation. Similarly, PABN-treated cells showed a continuous
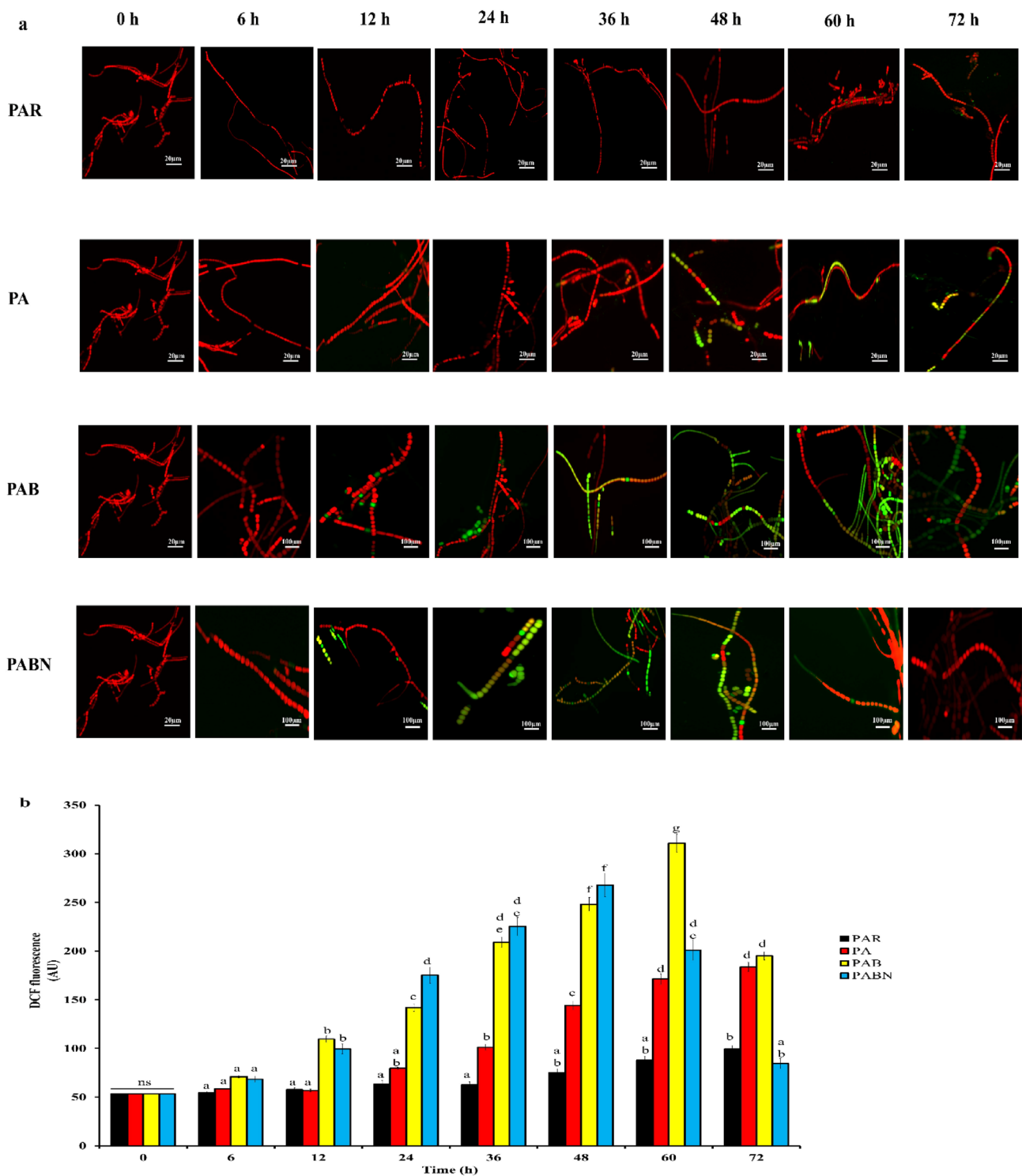
Fig. 4 Fluorescence images of PAR, PA, PAB, and PABN treated cells showing intracellular green 2′,7′-dichlorodihydrofluorescein (DCF) fluorescence following a different duration of exposure as a result of ROS production. The 0 h DCF fluorescence images were used as a control (**a**); Emission spectra of DCF fluorescence intensities following exposure to PAR, PA, PAB, and PABN during various exposure times (**b**). The standard deviation of the mean is shown by the error bar (means ± SD, $n = 3$). The presence of a horizontal line over the bars over treatments denotes no significant difference ($p > 0.05$). Tukey test in the range of $p < 0.05$ was used to evaluate the significance of data. Homogeneous mean groups are indicated by similar letters across the bars
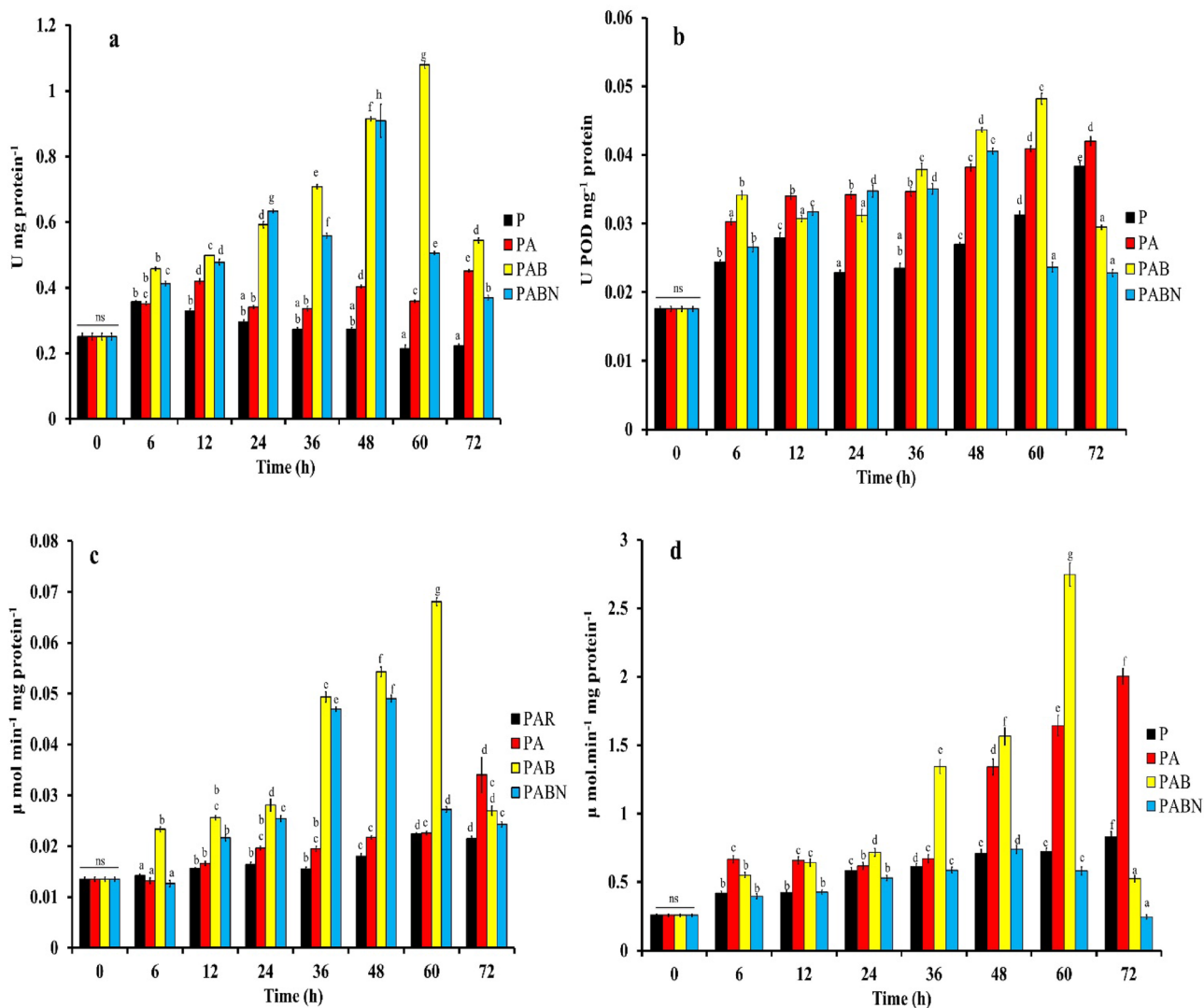
Fig. 5 Activity of antioxidative enzymes. SOD (U mg protein^{-1}) (**a**); POD (U POD mg^{-1} protein) (**b**); CAT (μ mol min^{-1} mg protein^{-1}) (**c**); APX (μ mol.min^{-1} mg protein^{-1}) (**d**), in *Nostochopsis lobatus* HKAR-21 subjected to PAR, PA, PAB, and PABN irradiation for varied time periods. The standard deviation of the mean is shown by the error bar (means $\pm$ SD, $n = 3$). The presence of a horizontal line and the bars over treatments denotes no significant difference ($p > 0.05$). Tukey test in the range of $p < 0.05$ was used to evaluate the significance of data. Homogeneous mean groups are indicated by similar letters across the bars

increase of 2.3-fold after 48 h of exposure. After 48 h, POD activity started to decline (Fig. 5b).

In control, CAT activity was 0.0135 ± 0.0004 μmol min^{-1} mg^{-1} protein; after 72 h of PAR exposure, this value marginally rose up to 1.6-fold (Fig. 5c). After 72 h of PA administration, there was a 2.5-fold ($p < 0.05$) induction of CAT activity, which increased steadily in response to PA exposure. Similar to how CAT activity increased after PAB exposure, maximal induction was seen at 60 h (i.e., 5 times) ($p < 0.05$) after treatment. A decrease in CAT activity resulted in more irradiation. However, only a slight increase in the CAT activity was observed (twofold) after 72 h of PABN treatment (Fig. 5c).

After 72 h of treatment, APX activity in samples that had received PAR rose but not significantly, and it remained nearly at the same level as in control samples (Fig. 5d). When compared to the control, APX activity increased considerably after exposure to PA and PAB. Up to 72 h of stimulation in PA, it was enhanced by 7.8-fold ($p < 0.05$). The APX activity under PAB also increased significantly ($p < 0.05$), peaking 10.6-fold after 60 h of treatment in comparison to the control. After exposure to PAB for 60 h, the activity was observed to have decreased. After 72 h of PABN administration, no appreciable rise in APX activity was seen; instead, it stayed at the same level as the control (Fig. 5d). Under UVR (PAB) stress, the examined cyanobacterium showed a

positive correlation between exposure time and physiological processes such as ROS production, SOD, POD, CAT, and APX activities. The action of SOD, POD, CAT, and APX against ROS production also showed a favorable connection. This could be the result of enhanced antioxidant enzyme activity in response to rising UVR exposure.

3.6 Lipid peroxidation

Lipid peroxidation measured as MDA content of *Nostochopsis lobatus* HKAR-21 irradiated with different periods of PAR, UV-A, UV-B and UVBN irradiation are shown in Fig. 6. The results high-lighted that after 72 h of PAR and PA irradiation, the MDA contents were increased by 0.209 (1.57 times) and 0.252 (1.69 times) nmol g^{-1} fresh weight respectively, as compared to the control. However, in PAB-irradiated samples, the highest increment of 1.73-fold in MDA content was found after 60 h of treatment as compared to the unirradiated control culture, but after 60 h, there was a slight decrease. Similarly, in PABN treated culture, the MDA contents were increased by 1.70-fold, as compared to the control but after 48 h of the incubation period, it decreased sharply (Fig. 6).

4 Discussion

Physiological and biochemical responses of organisms including those of cyanobacteria, are profoundly influenced by environmental variation. Incoming sun radiation is essential for cyanobacteria to carry out the processes of nitrogen

Fig. 6 Effect of different exposure time of UV radiation on MDA content (nmol. g^{-1} fresh weight) of Rice-field cyanobacterium *Nostochopsis lobatus* HKAR-21. The standard deviation of the mean is shown by the error bar (means ± SD, *n* = 3). The presence of a horizontal line and the bars over treatments denotes no significant difference (*p* > 0.05). Tukey test in the range of *p* < 0.05 was used to evaluate the significance of data. Homogeneous mean groups are indicated by similar letters across the bars

fixation and photosynthesis. Increasing salinity and UV-radiation are the two major abiotic factors that severely affect the photosynthetic efficiency and photopigments accessibility of many chlorophyllous organisms. The present study focused on studying the combined effect of salt (NaCl) and UV-radiation in rice field cyanobacterium *Nostochopsis lobatus* strain HKAR-21. The extensive salinity increment suppressed the photopigments activity and negatively affected the production of many other macromolecules of *Nostochopsis lobatus* strain HKAR-21. However, the inhibiting effect of NaCl was more pronounced at 200 mM concentration. In addition to salt, UV light causes photosynthetic pigments to fade while also impairing cyanobacterial photosynthesis quickly [63]. Additionally, it has a negative impact on the productivity, yields, and protein composition of many cyanobacterial species [64]. Because of the protein's absorbance range, it can be easily damaged by UV light [65]. Thus, these findings demonstrate that proteins are more vulnerable to PAB radiation than PAR and PA radiation. Numerous reports have highlighted that exposure to UV radiation decreases the effectiveness of the photosynthetic activity of cyanobacteria [18, 66]. Chronic photoinhibition is increased by the breakdown of PSII structural D1 proteins in response to strong UV light. [67].

The current study focuses on modifications in total proteins and photosynthetic pigments caused by PAR, PA, PAB, and PABN (Table 1). It has also been determined how changes in rETR, Y(NPQ), and Y(NO) (Fig. 3), as well as the activity of antioxidant enzymes (Fig. 5) like CAT, SOD, POD, and APX have affected the maximum quantum yield of PSII (F_V/F_M) of the cyanobacterium, as shown in Table 2. Additionally, the lipid peroxidation activity and free radicals (ROS) in living cells have been measured with the help of DCFH-DA dye. As shown in Table 1, UVR exposure time had a substantial impact on the photosynthetic pigment damage in *Nostochopsis*. It was also noted that the amount of the photosynthetic pigment Chl *a* changed depending on how long it was exposed to PAR, PA, PAB, and PABN. In contrast to PA, where Chl *a* increased more slowly, a large rise in Chl *a* was seen in PAR. However, cells exposed to PAB and PABN radiation showed a considerable reduction. Intense PAB and PABN exposure to photosynthetic pigments causes fast bleaching and suppresses photosynthetic activity in cyanobacteria [63]. This effect was more enhanced in PABN-irradiated cells due to the presence of salt, which increases the fluidity of the membrane and significantly helps UV-B radiation to breach the cyanobacterial cells. In terms of the overall carotene content, it can be shown that cells maintained under various exposure conditions produce much more carotene. As indicated in the Table 1, biggest rise in carotene level was seen in cells exposed to PA; Although, in PAB treated cells total carotene synthesis was significantly increased up to 48 h, after that
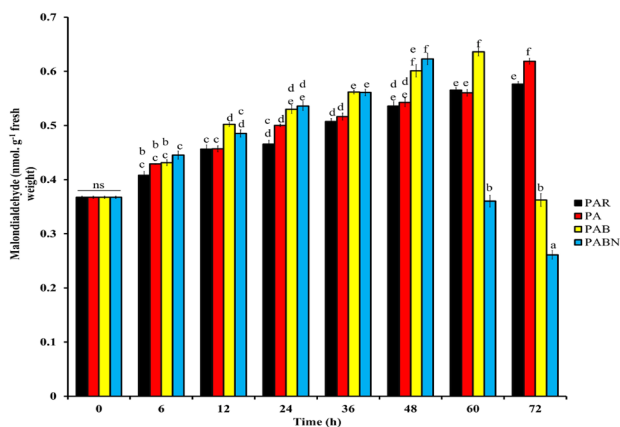
it begins to decline. This increment in the carotenes concentration was highlighted that carotenes are well-known photoprotective molecules having a strong capacity to scavenge ROS [68]. Similar results were found by Vincent and Quesada 1994 in *Aphanothece* sp., increased total carotene content as a result of UV-B exposure because of their function as singlet oxygen scavengers [69].

This study discovered that *Nostochopsis* exposed to PAB and PABN had significantly reduced photosynthetic efficiency (Table 2). The observed decline in *Nostochopsis*' photosynthetic capacity under UVR was consistent with other results that noted a decline in F_V/F_M under UVR in a number of cyanobacterial species [64, 70]. Although both UV-B and UV-A damage to PSII has similar effects, UV-A damage is often less severe [71]. Additionally, exposure to UV-B radiation can alleviate the stress and enhance the turnover of D1 and D2 proteins in the reaction center of PSII in cyanobacteria [72]. A few studies have shown the negative effects of UVR (long-term exposure with modest PAR and UVR) on photosynthetic performance and its recovery after damage [65]. Furthermore, our findings demonstrate that rETR in cells exposed to PAR, PA, PAB, and PABN differs considerably. rETR values rise with radiation exposure until they reach a saturation point, and they were lower in the samples exposed to PAB and PABN than those treated with PAR and PA, as shown in (Fig. 3a–d). The rETR increased steadily as exposure time to PAR and PA increased, showing a considerable improvement in the photosynthetic system's ability to transport electrons. However, when the actinic light irradiance of PAM rises, the cyanobacterium *Nostochopsis lobatus* HKAR-21 electron transport system becomes saturable, causing PAM to abruptly down-regulate. The quantum yield of PSII and rETR both responded similarly. However, in samples exposed to PAB radiation, rETR levels spiked for up to 6 h before steadily falling to their lowest point. After 60 h of irradiation, samples stored in PABN exhibited a considerable reduction in rETR, and it was discovered that cells' ability to transport electrons was entirely stopped.

Our study indicates that constant exposure to UV-radiation with salt shows a synergistic effect on the photosystem of cyanobacterium, and the electron transport channels of cells were affected severely, which results in the unsystematic or random movement of electrons [70]. Furthermore, in this study, increased Y(NO) (Fig. 3i-l) and decreased Y(NPQ) (Fig. 3e–h) of *Nostochopsis lobatus* HKAR-21 indicated that more absorbed energy flux was dissipated through non-regulated quenching mechanisms in PSII to prevent the over reduction of ETC in stressed *Nostochopsis lobatus* HKAR-21. This suggests that non-regulated heat dissipation plays an important acclimatory role in rice field cyanobacterium *Nostochopsis lobatus* HKAR-21 to protect the photosynthetic machinery from photo-inhibition under higher doses of UV-radiation and salt stress, with the

regulated heat dissipation playing possibly a less important role. Very similar findings in six cyanobacterial species were also reported by [73] under high-light conditions.

Continuous exposure to PAR, PA, PAB, and PABN revealed a considerable rise in the antioxidant enzymes needed to counteract the harmful effects of free radicals (Fig. 5) [74]. As reported earlier, In *Nostoc* sp. strain HKAR-2, it was discovered that the CAT, SOD, and APX activities were increased during the daily transient light and dark phases of PAR, UV-B, and PAR + UV-B [63]. The activity of CAT, SOD, and POD increased continuously during the light phase of PAR, PA, and PAB irradiation in *Anabaena siamensis* TISTR-8012, according to a similar finding by Rastogi et al. [26]. Similar to this, as shown in Fig. 5, our research discovered a multifold increase in antioxidative enzyme activity (i.e., SOD, POD, CAT, and APX) following PAB and PABN irradiation as compared to PAR. However, PAB-treated samples showed the greatest induction of all examined antioxidative enzymes. Our results agree with other studies on *Anabaena doliolum* by Singh et al. (2013) [70]. Additionally, prior research has demonstrated that UV-B radiation induces the transcripts of antioxidant enzyme systems [75]. Three cyanobacteria were shown to have increased SOD, CAT, and POD activity after being exposed to UV-B light for 15 and 60 min [76, 77]. The cyanobacterial cells are protected by the larger rise in the activity of the SOD, CAT, and POD defence mechanisms, which scavenge excessive ROS and protect PSII from increased UVR. By reducing Chl *a* bleaching, photoinhibition of photosynthesis, lipid peroxidation, and DNA damage after UVR exposure, exogenous antioxidant supplementation improved the survival rates of *Anabaena* sp. [27] and *Nostoc* sp. [78]. These results of antioxidant enzyme activity were clearly reinforced by the in vivo ROS increment in the cyanobacterial cells, which was clearly observed in fluorescence microscopy, (Fig. 4a) spectroscopy (Fig. 4b) and G/R ratio (Supplementary Fig. S1) of the cyanobacterium. There was an increase in MDA content after UV radiations in *Nostochopsis lobatus* HKAR-21 (Fig. 6). An increase in MDA contents is similar to results obtained by other investigators on *Chlorococcum* sp. [79] and *Anabaena* sp. [80]. This increase in MDA contents is due to the peroxidation of the membrane lipids due to increased ROS production during UV radiation [81].

5 Conclusion

Based on the findings of this research, it was demonstrated that salinity and UV-irradiation severely affect the major macromolecular components of the rice-field cyanobacterium *Nostochopsis lobatus* HKAR-21. Salt stress mainly causes impairment in the membrane, which negatively

impacts the cyanobacterial cell's osmotic balance. Results in depletion of major protein components and photopigments activity. UV radiation primarily affects the photosynthetic pigments, damages the electron transport rate, as well as negatively impacts the composition of the lipid membrane of the cyanobacterium. Compared with PAR, UV radiation significantly changes the flow of energy and the cyanobacterium dissipates electrons in a non-regulated manner. In PSII exposed to UVR, NPQ may be the primary mechanism for excessive energy dissipation, whereas photochemical quenching is essential in avoiding photoinhibition. These findings suggest that ROS production may play a role in the UVR-induced injury. To reduce ROS-induced oxidative stress, cyanobacteria have evolved effective antioxidant systems, which include antioxidant compounds like carotenoids and antioxidant enzymes like SOD, POD, CAT, and APX. Our study indicated that the cyanobacterium has many enzymatic and non-enzymatic strategies to cope with these increasing abiotic stresses. But, if this scenario continues to be like that, then it will severely impact the productivity of photosynthetic organisms like cyanobacteria. As cyanobacteria are the major contributors in rice production, their growth impairment will adversely impact the productivity of one of the most important crops on which more than a billion people are dependent. Therefore, extensive research is required in the field of abiotic stresses and their impacts on the photosynthetic ability of organisms like cyanobacteria. The molecular exploration of different genes involved in the resilience of stresses such as UVR are still a research area to be explored. Hence, efforts are required to reduce the soil salinity together with climate shift for the sustainable development of organisms.

Data availability The data of our research can be acquired from the Supplementary materials uploaded with this article.

Declarations

Conflict of interest The authors have no conflicts of interest to declare that are relevant to the content of this article.

References

1. Fischer, W. F. (2008). Life before the rise of oxygen. *Nature, 455*(7216), 1051–1052. https://doi.org/10.1038/4551051a
2. Pathak, J., Rajneesh, Maurya, P. K., Singh, S. P., Häder, D.-P., & Sinha, R. P. (2018). Cyanobacterial farming for environment friendly sustainable agriculture practices: innovations and perspectives. *Frontiers in Environmental Science, 6*, 7. https://doi.org/10.3389/fenvs.2018.00007
3. Whitton, B. A. (2012). Ecology of cyanobacteria II: Their Diversity In Space And Time. *Springer Science & Business Media, Dordrecht.* https://doi.org/10.1007/978-94-007-3855-3
4. Singh, N. K., Dhar, D. W., & Tabassum, R. (2016). Role of cyanobacteria in crop protection. *Proceedings of the National Academy of Sciences, India Section B: Biological Sciences, 86*, 1–8. https://doi.org/10.1007/s40011-014-0445-1
5. Prasanna, R., Jaiswal, P., & Kaushik, B. D. (2008). Cyanobacteria as potential options for environmental sustainability—promises and challenges. *Indian Journal of Microbiology, 48*, 89–94. https://doi.org/10.1007/s12088-008-0009-2
6. Das, N. P., Kumar, A., & Singh, P. K. (2015). Cyanobacteria, pesticides and rice interaction. *Biodiversity and Conservation, 24*, 995–1005. https://doi.org/10.1007/s10531-015-0886-8
7. Dash, N. P., Kumar, A., Kaushik, M. S., Abraham, G., & Singh, P. K. (2017). Agrochemicals influencing nitrogenase, biomass of N2-fixing cyanobacteria and yield of rice in wetland cultivation. *Biocatalysis and Agricultural Biotechnology, 9*, 28–34. https://doi.org/10.1016/j.bcab.2016.11.001
8. Sui, N., Wang, Y., Liu, S., Yang, Z., Wang, F., & Wan, S. (2018). Transcriptomic and physiological evidence for the relationship between unsaturated fatty acid and salt stress in peanut. *Frontiers in Plant Science, 9*, 7. https://doi.org/10.3389/fpls.2018.00007
9. Song, J., & Wang, B. (2015). Using euhalophytes to understand salt tolerance and to develop saline agriculture: *Suaeda salsa* as a promising model. *Annals of Botany, 115*(3), 541–553. https://doi.org/10.1093/aob/mcu194
10. Häder, D.-P., Williamson, C. E., Wängberg, S. Å., Rautio, M., Rose, K. C., Gao, K., Helbling, E. W., Sinha, R. P., & Worrest, R. (2015). Effects of UV radiation on aquatic ecosystems and interactions with other environmental factors. *Photochemical and Photobiological Sciences, 14*(1), 108–126. https://doi.org/10.1039/C4PP90035A
11. Burkholder, J. B., Cox, R. A., & Ravishankara, A. R. (2015). Atmospheric degradation of ozone depleting substances, their substitutes, and related species. *Chemical Reviews, 115*(10), 3704–3759. https://doi.org/10.1021/cr5006759
12. Li, W., & Li, Q. (2017). Effect of environmental salt stress on plants and the molecular mechanism of salt stress tolerance. *International Journal of Environmental Sciences and Natural Resources, 7*(3), 81–86.
13. Los, D. A., Zorina, A., Sinetova, M., Kryazhov, S., Mironov, K., & Zinchenko, V. V. (2010). Stress sensors and signal transducers in cyanobacteria. *Sensors, 10*(3), 2386–2415. https://doi.org/10.3390/s100302386

14. Klähn, S., Mikkat, S., Riediger, M., Georg, J., Hess, W. R., & Hagemann, M. (2021). Integrative analysis of the salt stress response in cyanobacteria. *Biology Direct, 16*(1), 26. https://doi.org/10.1186/s13062-021-00316-4

15. Jensen, P. E., & Leister, D. (2014). Cyanobacteria as an experimental platform for modifying bacterial and plant photosynthesis. *Frontiers in Bioengineering and Biotechnology, 2*, 7. https://doi.org/10.3389/fbioe.2014.00007

16. Rajneesh, Singh, S. P., Pathak, J., & Sinha, R. P. (2017). Cyanobacterial factories for the production of green energy and value-added products: An integrated approach for economic viability. *Renewable and Sustainable Energy Reviews, 69*, 578–595. https://doi.org/10.1016/j.rser.2016.11.110

17. Gutu, A., & Kehoe, D. M. (2012). Emerging perspectives on the mechanisms, regulation, and distribution of light color acclimation in cyanobacteria. *Molecular Plant, 5*(1), 1–13. https://doi.org/10.1093/mp/ssr054

18. Rastogi, R. P., Incharoensakdi, A., & Madamwar, D. (2014). Responses of a rice-field cyanobacterium *Anabaena siamensis* TISTR-8012 upon exposure to PAR and UV radiation. *Journal of Plant Physiology, 171*(16), 1545–1553. https://doi.org/10.1016/j.jplph.2014.07.011

19. Kehoe, D. M., & Gutu, A. (2006). Responding to color: The regulation of complementary chromatic adaptation. *Annual Review of Plant Biology, 57*, 127–150. https://doi.org/10.1146/annurev.arplant.57.032905.105215

20. Gupta, A., Singh, A. P., Singh, V. K., Singh, P. R., Jaiswal, J., Kumari, N., Upadhye, V., Singh, S. C., & Sinha, R. P. (2023). Natural sun-screening compounds and DNA-repair enzymes: Photoprotection and photoaging. *Catalysts, 13*(4), 745. https://doi.org/10.3390/catal13040745

21. Klisch, M., Sinha, R. P., Helbling, E. W., & Häder, D.-P. (2005). Induction of thymine dimers by solar radiation in natural freshwater phytoplankton assemblages in Patagonia, Argentina. *Aquatic Sciences, 67*(1), 72–78. https://doi.org/10.1007/s00027-004-0770-1

22. Sinha, R. P., & Häder, D.-P. (2002). UV-induced DNA damage and repair: A review. *Photochemical and Photobiological Sciences, 1*(4), 225–236. https://doi.org/10.1039/B201230H

23. Singh, P. R., Gupta, A., Pathak, J., & Sinha, R. P. (2023). Phylogenetic distribution, structural analysis and interaction of nucleotide excision repair proteins in cyanobacteria. *DNA Repair, 126*, 103487. https://doi.org/10.1016/j.dnarep.2023.103487

24. Rastogi, R. P., Singh, S. P., Häder, D.-P., & Sinha, R. P. (2011). Ultraviolet-B-induced DNA damage and photorepair in the cyanobacterium *Anabaena variabilis* PCC 7937. *Environmental and Experimental Botany, 74*, 280–288. https://doi.org/10.1016/j.envexpbot.2011.06.010

25. Rajneesh, P., & J., Häder, D.-P., & Sinha, R.P. (2019). Impacts of ultraviolet radiation on certain physiological and biochemical processes in cyanobacteria inhabiting diverse habitats. *Environmental and Experimental Botany, 161*, 375–387. https://doi.org/10.1016/j.envexpbot.2018.10.037

26. Rastogi, R. P., Sinha, R. P., Moh, S. H., Lee, T. K., Kottuparambil, S., Kim, Y. J., Rhee, J. S., Choi, E. M., Brown, M. T., Häder, D.-P., & Han, T. (2014). Ultraviolet radiation and cyanobacteria. *Journal of Photochemistry and Photobiology B: Biology, 141*, 154–169. https://doi.org/10.1016/j.jphotobiol.2014.09.020

27. He, Y. Y., & Häder, D.-P. (2002). UV-B-induced formation of reactive oxygen species and oxidative damage of the cyanobacterium *Anabaena* sp.: Protective effects of ascorbic acid and N-acetyl-L-cysteine. *Journal of Photochemistry and Photobiology B: Biology, 66*(2), 115–124. https://doi.org/10.1016/S1011-1344(02)00231-2

28. Thapar, R., Srivastava, A. K., Bhargava, P., Mishra, Y., & Rai, L. C. (2008). Impact of different abiotic stresses on growth, photosynthetic electron transport chain, nutrient uptake and enzyme activities of Cu-acclimated *Anabaena doliolum*. *Journal of Plant Physiology, 165*(3), 306–316. https://doi.org/10.1016/j.jplph.2007.05.002

29. Barbato, R., Bergo, E., Szabò, I., Dalla Vecchia, F., & Giacometti, G. M. (2000). Ultraviolet B exposure of whole leaves of barley affects structure and functional organization of photosystem II. *Journal of Biological Chemistry, 275*(15), 10976–10982. https://doi.org/10.1074/jbc.275.15.10976

30. Tyystjärvi, E. (2008). Photoinhibition of photosystem II and photodamage of the oxygen evolving manganese cluster. *Coordination Chemistry Reviews, 252*(3–4), 361–376. https://doi.org/10.1016/j.ccr.2007.08.021

31. Singh, A., Sarkar, A., Singh, S., & Agrawal, S. B. (2010). Investigation of supplemental ultraviolet-B-induced changes in antioxidative defense system and leaf proteome in radish (*Raphanus sativus* L. cv Truthful): An insight to plant response under high oxidative stress. *Protoplasma, 245*, 75–83. https://doi.org/10.1007/s00709-010-0138-4

32. Barufi, J. B., Korbee, N., Oliveira, M. C., & Figueroa, F. L. (2011). Effects of N supply on the accumulation of photosynthetic pigments and photoprotectors in *Gracilaria tenuistipitata* (Rhodophyta) cultured under UV radiation. *Journal of Applied Phycology, 23*, 457–466. https://doi.org/10.1007/s10811-010-9603-x

33. Roleda, M. Y., Nyberg, C. D., & Wulff, A. (2012). UVR defense mechanisms in eurytopic and invasive *Gracilaria vermiculophylla* (Gracilariales, Rhodophyta). *Physiologia Plantarum, 146*(2), 205–216. https://doi.org/10.1111/j.1399-3054.2012.01615.x

34. Figueroa, F. L., Conde-Alvarez, R., & Gómez, I. (2003). Relations between electron transport rates determined by pulse amplitude modulated chlorophyll fluorescence and oxygen evolution in macroalgae under different light conditions. *Photosynthesis Research, 75*, 259–275. https://doi.org/10.1023/A:1023936313544

35. Rippka, R., Deruelles, J., Waterbury, J. B., Herdman, M., & Stanier, R. Y. (1979). Generic assignments, strain histories and properties of pure cultures of cyanobacteria. *Microbiology, 111*(1), 1–61. https://doi.org/10.1099/00221287-111-1-1

36. Altschul, S. F., Gish, W., Miller, W., Myers, E. W., & Lipman, D. J. (1990). Basic local alignment search tool. *Journal of Molecular Biology, 215*(3), 403–410. https://doi.org/10.1016/S0022-2836(05)80360-2

37. Desikachary, T. V. (1959). *Cyanophyta*. Indian Council of Agriculture Research.

38. Saitou, N., & Nei, M. (1987). The neighbor-joining method: A new method for reconstructing phylogenetic trees. *Molecular Biology and Evolution, 4*(4), 406–425. https://doi.org/10.1093/oxfordjournals.molbev.a040454

39. Kumar, S., Stecher, G., & Tamura, K. (2016). MEGA7: molecular evolutionary genetics analysis version 7.0 for bigger datasets. *Molecular Biology and Evolution, 33*(7), 1870–1874. https://doi.org/10.1093/molbev/msw054

40. Lowry, O. H., Rosebrough, N. J., Farr, A. L., & Randall, R. J. (1951). Protein measurement with the Folin phenol reagent. *Journal of Biological Chemistry, 193*(1), 265–275.

41. Şükran, D., Güneş, T., & Sivaci, R. (1998). Spectrophotometric determination of chlorophyll-*a*, *b* and total carotenoid contents of some algae species using different solvents. *Turkish Journal of Botany, 22*(1), 13–18.

42. Kannaujiya, V. K., & Sinha, R. P. (2016). An efficient method for the separation and purification of phycobiliproteins from a rice-field cyanobacterium *Nostoc* sp. strain HKAR-11. *Chromatographia, 79*(5–6), 335–343. https://doi.org/10.1007/s10337-016-3025-0

43. Bennett, A., & Bogorad, L. (1973). Complementary chromatic adaptation in a filamentous blue-green alga. *The Journal of cell biology, 58*(2), 419–435. https://doi.org/10.1083/jcb.58.2.419

44. Ryckebosch, E., Muylaert, K., & Foubert, I. (2012). Optimization of an analytical procedure for extraction of lipids from microalgae. *Journal of the American Oil Chemists' Society, 89*(2), 189–198. https://doi.org/10.1007/s11746-011-1903-z

45. DuBois, M., Gilles, K. A., Hamilton, J. K., Rebers, P. T., & Smith, F. (1956). Colorimetric method for determination of sugars and related substances. *Analytical Chemistry, 28*(3), 350–356. https://doi.org/10.1021/ac60111a017

46. Kitajima, M. B. W. L., & Butler, W. L. (1975). Quenching of chlorophyll fluorescence and primary photochemistry in chloroplasts by dibromothymoquinone. *Biochimica et Biophysica Acta (BBA)-Bioenergetics, 376*(1), 105–115. https://doi.org/10.1016/0005-2728(75)90209-1

47. Genty, B., Briantais, J. M., & Baker, N. R. (1989). The relationship between the quantum yield of photosynthetic electron transport and quenching of chlorophyll fluorescence. *Biochimica et Biophysica Acta (BBA)-General Subjects, 990*(1), 87–92. https://doi.org/10.1016/S0304-4165(89)80016-9

48. Cailly, A.L., Rizza, F., Genty. B., & Harbinson. J. (1996) Fate of excitation at PS II in leaves. The non-photochemical side. *Plant Physiology and Biochemistry 86*.

49. Kramer, D. M., Johnson, G., Kiirats, O., & Edwards, G. E. (2004). New fluorescence parameters for the determination of QA redox state and excitation energy fluxes. *Photosynthesis Research, 79*, 209–218. https://doi.org/10.1023/B:PRES.0000015391.99477.0d

50. Srivastava, A., Biswas, S., Yadav, S., Kumar, A., Rajaram, H., Srivastava, V., & Mishra, Y. (2021). Physiological and thylakoid proteome analyses of *Anabaena* sp. PCC 7120 for monitoring the photosynthetic responses under cadmium stress. *Algal Research, 54*, 102225. https://doi.org/10.1016/j.algal.2021.102225

51. Rascher, U., Lakatos, M., Büdel, B., & Lüttge, U. (2003). Photosynthetic field capacity of cyanobacteria of a tropical inselberg of the Guiana Highlands. *European Journal of Phycology, 38*(3), 247–256. https://doi.org/10.1080/0967026031000121679

52. Klughammer, C., & Schreiber, U. (2008). Complementary PS II quantum yields calculated from simple fluorescence parameters measured by PAM fluorometry and the Saturation Pulse method. *PAM Application Notes, 1*(2), 201–247.

53. Tripathi, S.N., & Srivastava, P. (2001). Presence of stable active oxygen scavenging enzymes superoxide dismutase, ascorbate peroxidase and catalase in a desiccation-tolerant cyanobacterium *Lyngbya arboricola* under dry state. *Current Science*, 197–200. https://www.jstor.org/stable/24106259

54. Aebi, H. (1984). Catalase in vitro. In *Methods in enzymology* (Vol. 105, pp. 121–126). Academic press. https://doi.org/10.1016/S0076-6879(84)05016-3

55. Halliwell, B. (2006). Reactive species and antioxidants. Redox biology is a fundamental theme of aerobic life. *Plant Physiology, 141*(2), 312–322. https://doi.org/10.1104/pp.106.077073

56. Beauchamp, C., & Fridovich, I. (1971). Superoxide dismutase: Improved assays and an assay applicable to acrylamide gels. *Analytical Biochemistry, 44*(1), 276–287. https://doi.org/10.1016/0003-2697(71)90370-8

57. Britton, C., & Mehley, A. C. (1955). Assay of catalase and peroxidase. In S. P. Colowick & N. O. Kalpan (Eds.), *Method in enzymology* (pp. 764–775). Academic.

58. Nakano, Y., & Asada, K. (1981). Hydrogen peroxide is scavenged by ascorbate-specific peroxidase in spinach chloroplasts. *Plant and Cell Physiology, 22*(5), 867–880. https://doi.org/10.1093/oxfordjournals.pcp.a076232

59. Kampfenkel, K., Vanmontagu, M., & Inzé, D. (1995). Extraction and determination of ascorbate and dehydroascorbate from plant tissue. *Analytical Biochemistry, 225*(1), 165–167. https://doi.org/10.1006/abio.1995.1127

60. Heath, R. L., & Packer, L. (1968). Photoperoxidation in isolated chloroplasts: I. Kinetics and stoichiometry of fatty acid peroxidation. *Archives of Biochemistry and Biophysics, 125*(1), 189–198. https://doi.org/10.1016/0003-9861(68)90654-1

61. Singh, D. K., Pathak, J., Pandey, A., Rajneesh, Singh, V., & Sinha, R. P. (2022). Purification, characterization and assessment of stability, reactive oxygen species scavenging and antioxidative potentials of mycosporine-like amino acids (MAAs) isolated from cyanobacteria. *Journal of Applied Phycology, 34*(6), 3157–3175. https://doi.org/10.1007/s10811-022-02832-w

62. Kumari, N., Pandey, A., Gupta, A., Mishra, S., & Sinha, R. P. (2023). Characterization of UV-screening pigment scytonemin from cyanobacteria inhabiting diverse habitats of Varanasi, India. *Biologia, 78*(2), 319–330. https://doi.org/10.1007/s11756-022-01190-9

63. Kannaujiya, V. K., & Sinha, R. P. (2017). Impacts of diurnal variation of ultraviolet-B and photosynthetically active radiation on phycobiliproteins of the hot-spring cyanobacterium *Nostoc* sp. strain HKAR-2. *Protoplasma, 254*, 423–433. https://doi.org/10.1007/s00709-016-0964-0

64. Fragoso, G. M., Neale, P. J., Kana, T. M., & Pritchard, A. L. (2014). Kinetics of photosynthetic response to ultraviolet and photosynthetically active radiation in *Synechococcus* WH 8102 (Cyanobacteria). *Photochemistry and Photobiology, 90*(3), 522–532. https://doi.org/10.1111/php.12202

65. Karsten, U., Lembcke, S., & Schumann, R. (2007). The effects of ultraviolet radiation on photosynthetic performance, growth and sunscreen compounds in aeroterrestrial biofilm algae isolated from building facades. *Planta, 225*, 991–1000. https://doi.org/10.1007/s00425-006-0406-x

66. Sinha, R. P., Barbieri, E. S., Lebert, M., Helbling, E. W., & Häder, D.-P. (2003). Effects of solar radiation on phycobiliproteins of marine red algae. *Trends in Photochemistry and Photobiology, 10*, 149–157.

67. Sinha, R. P., Helbling, E. W., & Häder, D.-P. (2003). Effects of solar radiation on photosynthetic quantum yield of a cyanobacterium *Nostoc* sp. *Trends in Photochemistry and Photobiology, 10*, 159–166.

68. Pattanaik, B., Roleda, M. Y., Schumann, R., & Karsten, U. (2008). Isolate-specific effects of ultraviolet radiation on photosynthesis, growth and mycosporine-like amino acids in the microbial mat-forming cyanobacterium *Microcoleus chthonoplastes*. *Planta, 227*, 907–916. https://doi.org/10.1007/s00425-007-0666-0

69. Vincent, W. F., & Quesada, A. (1994). Ultraviolet radiation effects on cyanobacteria: implication for Antarctic microbial ecosystems. In C. S. Weiler & P. A. Penhale (Eds.), *Antarctic research series: ultraviolet radiation in Antarctica: Measurements and biological effects* (pp. 111–124). American Geophysical Union. https://doi.org/10.1029/AR062p0111

70. Singh, S. P., Rastogi, R. P., Sinha, R. P., & Häder, D.-P. (2013). Photosynthetic performance of *Anabaena variabilis* PCC 7937 under simulated solar radiation. *Photosynthetica, 51*, 259–266. https://doi.org/10.1007/s11099-013-0012-7

71. Vass, I. (2012). Molecular mechanisms of photodamage in the Photosystem II complex. *Biochimica et Biophysica Acta (BBA)-Bioenergetics, 1817*(1), 209–217. https://doi.org/10.1016/j.bbabio.2011.04.014

72. Sass, L., Spetea, C., Máté, Z., Nagy, F., & Vass, I. (1997). Repair of UV-B induced damage of Photosystem II via de novo synthesis of the D1 and D2 reaction centre subunits in *Synechocystis* sp. PCC 6803. *Photosynthesis Research, 54*, 55–62. https://doi.org/10.1023/A:1005895924892

73. Misumi, M., Katoh, H., Tomo, T., & Sonoike, K. (2016). Relationship between photochemical quenching and non-photochemical quenching in six species of cyanobacteria reveals species difference in redox state and species commonality in energy dissipation. *Plant and Cell Physiology, 57*(7), 1510–1517. https://doi.org/10.1093/pcp/pcv185

74. Latifi, A., Ruiz, M., & Zhang, C. C. (2009). Oxidative stress in cyanobacteria. *FEMS Microbiology Reviews, 33*(2), 258–278. https://doi.org/10.1111/j.1574-6976.2008.00134.x

75. Singh, S. P., Häder, D.-P., & Sinha, R. P. (2010). Cyanobacteria and ultraviolet radiation (UVR) stress: Mitigation strategies. *Ageing Research Reviews, 9*(2), 79–90. https://doi.org/10.1016/j.arr.2009.05.004

76. Zeeshan, M., & Prasad, S. M. (2009). Differential response of growth, photosynthesis, antioxidant enzymes and lipid peroxidation to UV-B radiation in three cyanobacteria. *South African Journal of Botany, 75*(3), 466–474. https://doi.org/10.1016/j.sajb.2009.03.003

77. Singh, P. R., Pathak, J., Rajneesh, Ahmed, H., Häder, D.-P., & Sinha, R. P. (2023). Physiological responses of the cyanobacterium *Synechocystis* sp. PCC 6803 under rhythmic light variations. *Photochemical and Photobiological Sciences*. https://doi.org/10.1007/s43630-023-00429-x

78. Wang, G., Chen, K., Chen, L., Hu, C., Zhang, D., & Liu, Y. (2008). The involvement of the antioxidant system in protection of desert cyanobacterium . sp against UV-B radiation and the effects of exogenous antioxidants. *Ecotoxicology and Environmental Safety, 69*(1), 150–157. https://doi.org/10.1016/j.ecoenv.2006.03.014

79. Abo-Shady, A. M., El-Sheekh, M. M., El-Naggar, A. H., & Abomohra, A. E. F. (2008). Effect of UV-B radiation on growth, photosynthetic activity and metabolic activities of *Chlorococcum* sp. *Annals of Microbiology, 58*, 21–27. https://doi.org/10.1007/BF03179440

80. He, Y. Y., Klisch, M., & Häder, D.-P. (2002). Adaptation of cyanobacteria to UV-B stress correlated with oxidative stress and oxidative damage. *Photochemistry and Photobiology, 76*(2), 188–196. https://doi.org/10.1562/0031-8655(2002)0760188AOCTUB2.0.CO2

81. Huang, H., Ge, Z., Limwachiranon, J., Li, L., Li, W., & Luo, Z. (2017). UV-C treatment affects browning and starch metabolism of minimally processed lily bulb. *Postharvest Biology and Technology, 128*, 105–111. https://doi.org/10.1016/j.postharvbio.2017.02.010